Geological Society of Malaysia Bulletin 51
June 2005 p.95-101

Highly evolved S type granite : Selim Granite, Main Range Batholith, Peninsular Malaysia

Azman A Ghani

Department of Geology
University of Malaya
50603 Kuala Lumpur

Abstract: The Selim granite consists of coarse grained porphyritic biotite granite to medium to fine grained granite. Both granites overlap in many of the major element contents especially SiO2. The coarse grained porphyritic biotite granite has higher Fe2O3 and Na2O and has lower FeO compared to the medium to fine grained granite. Ba and Rb increases from the coarse grained porphyritic granite to equigranular medium to fine grained granite. Both granites are controlled by the same mineral assemblage during magmatic evolution that is K-feldspar, plagioclase and biotite. REE profile show that both granites may represent the evolved part of the Western Belt Granite. In all patterns, four elemental groups (La–Nd, Nd–Gd, Gd–Er, Er–Lu) form four distinct convex patterns. This pattern also known as tetrad REE effects, are not observed in common rock types, but are well documented in highly differentiated rocks with strong hydrothermal interaction (including pegmatite). The tetrad effect develops parallel to granite evolution, and significant tetrad effects are strictly confined to highly differentiated samples. The strong decrease of Eu concentrations in highly evolved rocks suggests that Eu fractionates between the residual melt and a coexisting aqueous high-temperature fluid. The effect has been progressively recognized, particularly for granitic rocks which have undergone high degree of fractional crystallisation, hydrothermal alteration and mineralization This feature is magmatic, inherited from crystallization of melt with the tetrad effect already produced and hardly be formed by post-magmatic water–rock interaction.

INTRODUCTION

The Western Belt granites of Peninsular Malaysia have been considered as constituting an exclusively 'S' type granites (e.g. Liew, 1983; Hutchison, 1996). The 'S' type features in the granites are, (a) high initial $^{87}Sr/^{86}Sr$ isotope ratio - > 0.710, (b) low Na_2O content, < 3.2% Na_2O in rocks with ~ 5% K_2O, (c) narrow range of felsic rock (SiO_2: 65.95 to 77.4%), (d) high K_2O/Na_2O ratio, 1.4 - 2.8 ('S' type rocks of the Lachlan Fold Belt : 0.9 - 3.2), (e) usually ilmenite bearing and (f) contain pelitic or quartzose metasedimentary xenoliths (Chappell and White 1992). Throughout the region Cobbing et al. (1992) found that many granite units distinguished on the basis of their primary textures commonly have variants with a secondary magmatic textures distinguished as two phased granitoids). They suggest that the latter resulted from the infiltration and disruption of coarse grained granite by granite fluids which crystallized to a fine grained equigranular mosaic texture. This paper will study in detail the geochemistry, particularly the significant of REE content in the Selim granite. The granite is part of the four granitic bodies which has been identified along the new Pos Selim to Kampung Raja highway, Perak. Preliminary granite mapping along the highway indicate that the main body of the Selim granite consists of two units, that is, coarse grained porphyritic biotite granite graded into equigranular medium to fine grained biotite granite. Emphasize will be given to the evolved nature of the Selim granite magma using the major, trace and REE elements composition.

GENERAL GEOLOGY AND PETROLOGY

The study area is located along the Pos Selim highway, Perak-Pahang border. The highway is part of the East West Highway project which is currently under construction. It stretches from Pos Selim in Perak to Ladang Blue Valley in Pahang and Kuala Berang in Terengganu. The Selim pluton crops from km 0 to km 3.4 of the highway. The pluton consists of coarse grained porphyritic biotite granite and medium to fine grained granite. The latter intruded by numerous tourmaline and aplite veins and dykes. The porphyritic biotite granite exposed from km 0 to km 1.1, usually weakly foliated with phenocrystic K-feldspar trending parallel to each other. The medium to fine grained granite varies gradationally from medium grained granite to fine grained granite, both granites characterized by blue coloured quartz. Intensity of both aplite and tourmaline veins and dykes also increases towards the centre of the pluton. The medium to fine grained granite are more equigranular and contain less ferromagnesium minerals compared to the outer porphyritic granite.

PETROGRAPHY

Coarse grained porphyritic biotite granite

The porphyritic Selim granite is characterized by large phenocryts with the size ranging from 5 to 8 cm and phenocryst-matrix ratio is about 50:50. Mineralogy of the granite in decreasing abundance is K-feldspar, quartz,

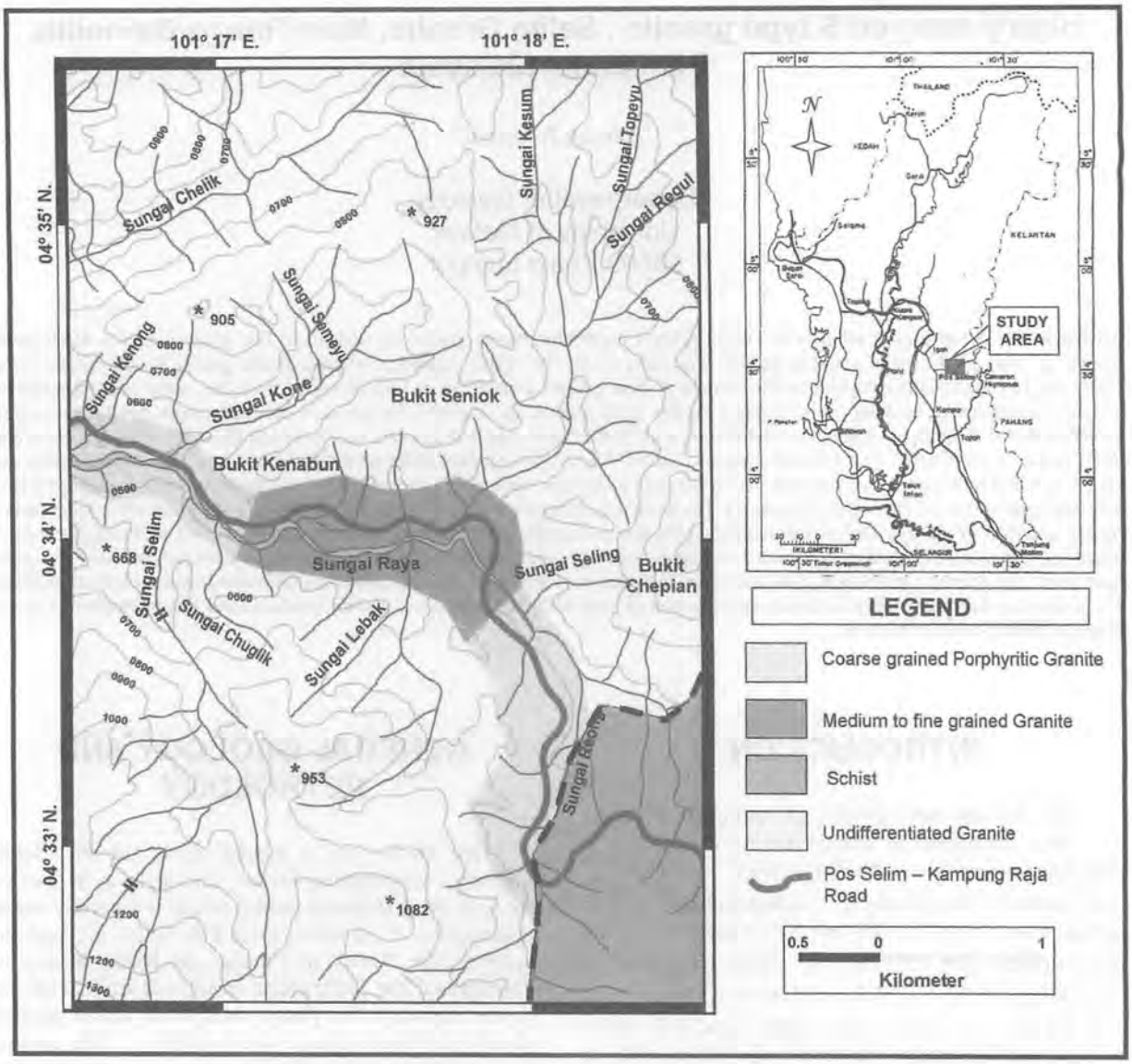

FIGURE 1: Geologic map of the Selim granite along the Pos Selim Kampung Raja Highway.

plagioclase, biotite, muscovite, apatite, secondary epidote and tourmaline. Large K-feldspar phenocrysts up to 7 cm long are common. The phenocrysts usually consist of microcline microperthite.

Plagioclases ranging from 0.7 to 4 mm in size and may occur as discrete phenocrysts or as glomeroporphyritic aggregate showing resorbed outlines in the mafic members of the granites. Quartz in the porphyritic granite is mostly anhedral and sometimes occurs as subgrains with the size ranging from 1 to 3 mm. Biotite occur as discrete plates, as ragged shreds in mafic clots and as small flakes associated with granoblastic aggregates of quartz and plagioclase. The pleochroism scheme is typically pale to dark brown but the green varieties also occur. Muscovite occurs as texturally secondary flakes usually resulting from alteration of plagioclase and K-feldspar. Tourmaline commonly occurs as interstitial skeletal network, which are most apparent in leucogranitic composition.

Medium to fine grained granite

This medium to fine grained granite is different from coarse grained porphyritic biotite granite by their phenocrysts with the size up to 5 mm and phenocryst-matrix ratio is about 10:90. Mineralogy of the granite is K-feldspar, quartz, plagioclase, biotite, secondary muscovite, apatite, secondary epidote and tourmaline. K-feldspar consists of microcline microperthite, ranging from 0.5 to 2.5 mm in size and from subhedral to anhedral in shape. Plagioclase is less abundance than K-feldspar with the same range in size and shape. Quartz is mostly anhedral with two obvious sizes, less than 1 mm and more than 1 mm. The latter usually form phenocrysts and occasionally contain apatite inclusions. Biotite occurs as small flake associated with granoblastic aggregates of quartz and plagioclase in small percentages (<10%) with secondary muscovite. The pleochroism scheme is typically pale to dark brown and occasionally contains

zircon and opaque inclusions with pleochroic rim. Tourmaline occurs as an individual mineral which are most apparent as inclusions in K-feldspar.

GEOCHEMISTRY

Sixteen samples (10 coarse grained porphyritic biotite granite and 6 equigranular medium to fine grained biotite granite) from the newly built road across the Selim granite were analysed for major, trace and rare earth elements (Table 1). The silica content of the coarse grained porphyritic biotite granite and equigranular medium to fine grained granite are overlap, 74.26 – 76.89 % SiO2 and 75.35 – 77.12 % SiO2 respectively. Harker diagrams for the
major and trace element oxides of the Selim granite are shown in Figure 2 and 3 respectively. Generally the equigranular medium to fine grained granite has lower TiO_2, FeO, MgO, K_2O, Ba and Sr and higher Fe_2O_3, Na_2O, Rb and Pb compared to the coarse grained porphyritic biotite granite.

The decrease of Ba concomitant with Sr as illustrated in Figure 4 suggests that K-feldspar, biotite and plagioclase are being removed in differentiation sequence for both coarse grained porphyritic granite and equigranular medium to fine grained granite. Rb/Sr ratio (Fig 5) for the equigranular medium to fine grained granite (inner unit) is higher than coarse grained porphyritic granite (outer unit). This suggests that the inner unit is more evolved compared to the outer units. The importance of K-feldspar, biotite and plagioclase in the differentiation is consistent with large ion lithophile (LIL) modelling. Inter-element LIL variation diagram for pairs Ba-Sr is shown in Figure 6. Also shown in each of the diagram is the vector diagram representing the net change in composition of the liquid after 30% Rayleigh fractionation by removing K-feldspar, hornblende, plagioclase or biotite. The trends are consistent with fractionation of plagioclase, K-feldspar and biotite. Thus the LIL log-log plot suggests that crystal fractionation plays an important role in the magmatic evolution of the Selim granite magma (cf Azman 2000a, b). REE pattern of the Selim granite are shown in Figure 7. All analysed samples show erratic LREE pattern, extreme negative Eu anomaly and variable HREE content. Both HREE and LREE do not have any specific trend with SiO2. All of the samples show tetrad REE patterns with huge negative anomalies. In all individual patterns, four elemental groups (La–Nd, Nd–Gd, Gd–Er, Er–Lu) form four distinct convex patterns. Tetrad REE effects are not observed in common rock types, but are well documented in highly differentiated rocks with strong hydrothermal interaction (including pegmatite). Irber (1999) showed that the tetrad effect develops parallel to granite evolution, and significant tetrad effects are strictly confined to highly differentiated samples. The strong decrease of Eu concentrations in highly evolved rocks suggests that Eu fractionates between the residual melt and a coexisting aqueous high-temperature fluid. This distinct trace element behavior and the common features of magmatic-hydrothermal alteration suggest the increasing importance of an aqueous-like fluid system during the final stages of granite crystallization.

CONCLUDING REMARKS

The Selim Granite is one of the examples of highly evolved granite in the Western Belt of Peninsular Malaysia. The rock is characterized by high silica content (SiO2 > 75%). Liew (1983) showed that the rocks with 75% SiO2 from the Western Belt Granite showed several characteristic features. Among them are high Rb (> 500 ppm), low Sr (< 50 ppm), Ba (<50 ppm) and Zr (< 125 ppm). They are enriched with Rb, U, Sn, Cs, Na, P, Nb, Ga, Mn, Be, B, F and Li and also show a rapid increase in abundance of elements like Rb, U, Sn and Sc with little change in major elements chemistry. The Selim Granite is one of the examples of high SiO2 granite from this region. Apart from having similar chemical characteristic to the highly evolved granites, this study also shows that the Selim Granite has a wonderful example of the REE tetrad effect (Fig 7) (Ludington 1981; Liggett 1990; Irber 1999; Jahn 2001). The chondrite-normalized abundances show relatively flat REE patterns with huge negative Eu anomalies. This is the characteristic REE tetrad effect, which is not observed in common rock types, but is well demonstrated in highly differentiated rocks with strong hydrothermal interaction (pegmatites included). The lanthanide tetrad effect has been progressively recognized, particularly for granitic rocks which have undergone high degree of fractional crystallisation, hydrothermal alteration and mineralization (Zhao et al., 1993; Lee et al., 1994, Bau, 1996; Irber, 1999). Rocks of similar geochemical characteristics have been published but their tetrad phenomena were passed unremarked. These include: the tourmaline granite of Harney Peak, Black Hills, South
Dakoda (Yurimoto et al., 1990), the Xihuashan granites in Jiangxi Province, China (Marue´jol et al., 1990) and the Suzhou A-type granite in Jiangsu Province, China (Charoy and Raimbault, 1994). The REE tetrad effect is most visible in late magmatic differentiates with strong hydrothermal interactions or deuteric alteration. This includes highly evolved leucogranites, pegmatites and mineralized granites. Such behavior occurs typically in highly evolved magmatic systems which are rich in H2O, CO2 and elements such as Li, B, F and/or Cl, and which may be regarded as transitional between a pure silicate melt and an aqueous fluid (e.g., London, 1986, 1987; Bau, 1996).

The celebrated negative Eu anomalies (> 95% Eu depletion) cannot be solely interpreted as due to feldspar separation although it is commonly known to have large positive Eu anomaly in its REE distribution coefficients. The primary cause of the tetrad effect, i.e., magma–fluid interaction, has not only severely depleted Eu in the rock, but also resulted in unusual negative Eu anomalies in all constituent minerals including K-feldspars (Zhao et al., 1999). It is possible that the fluid of either origin would, when interacted with highly evolved melt, lead to such trace element behavior. A second important question concerns whether post-magmatic water–rock interaction may also produce the same effect.

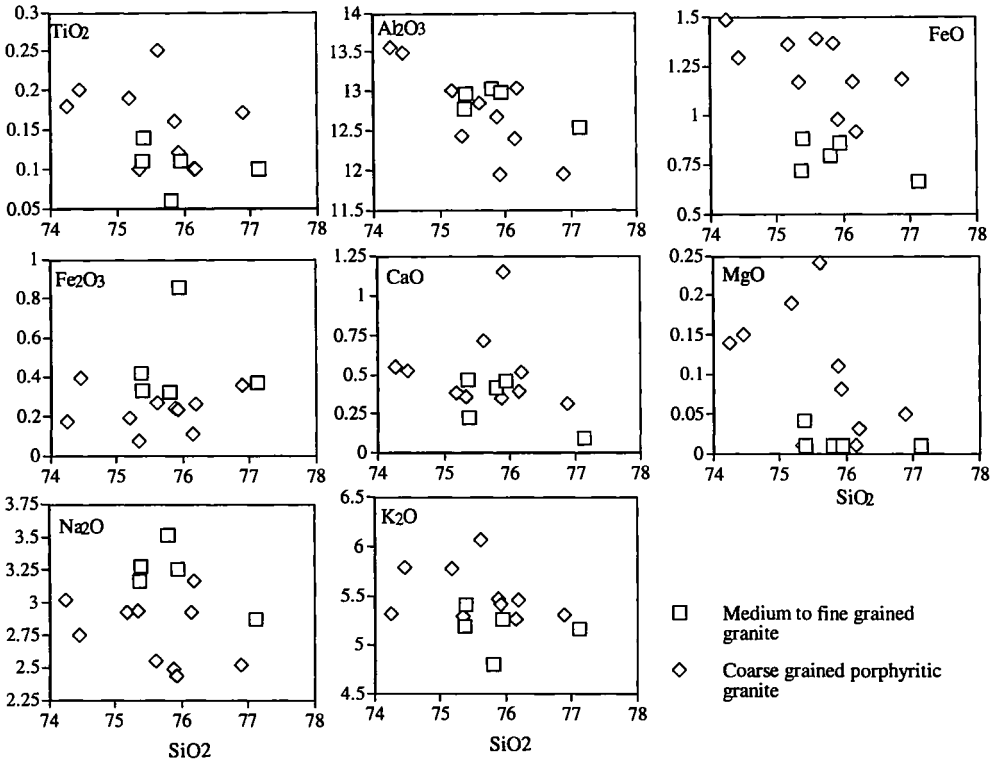

FIGURE 2: Harker diagrams for the major and minor element oxides

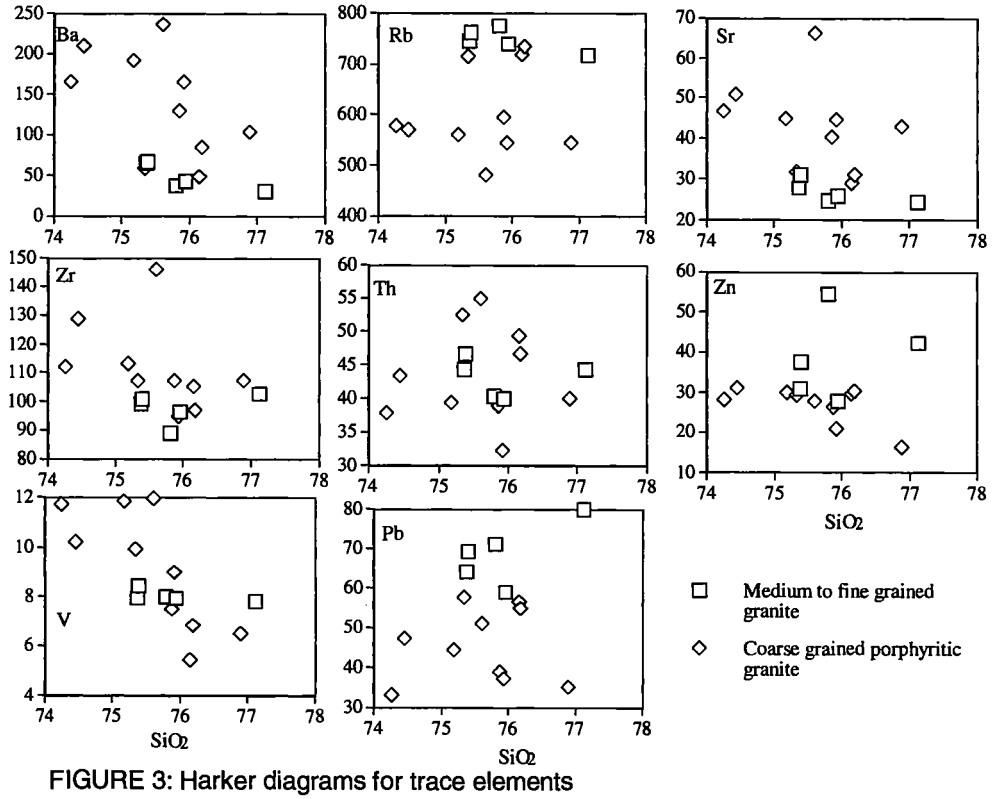

FIGURE 3: Harker diagrams for trace elements

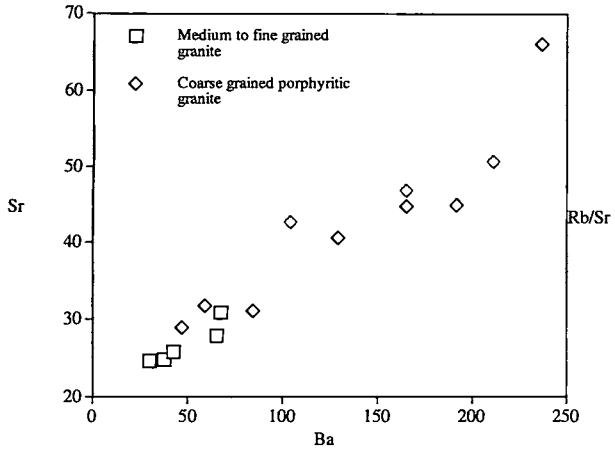

FIGURE 4 Ba vs Sr diagram of the Selim Granite. Note decreases of Ba concomitant with Sr indicate that influence of both K-feldspar and plagioclase in magmatic evolution.

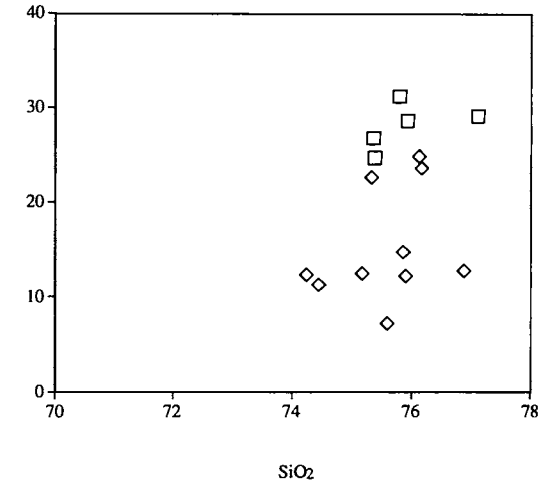

FIGURE 5: Rb/Sr vs SiO_2 diagram for the Selim granite.

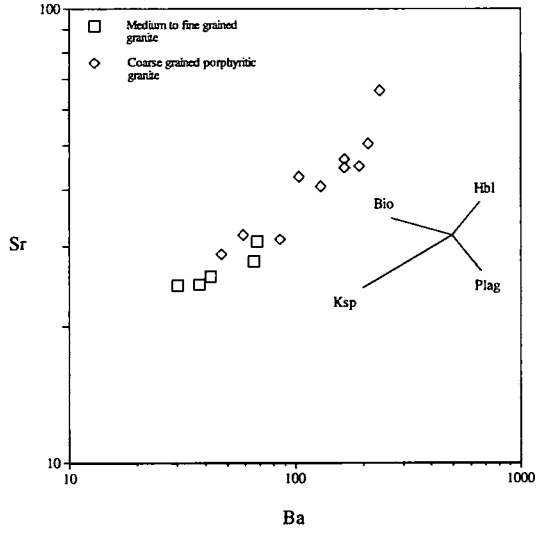

FIGURE 6: Ba vs Sr log plot for the Selim granite. Note that both granites (porphyritic and fine to medium grained granite) controlled by the same mineral assemblage during the magmatic evolution

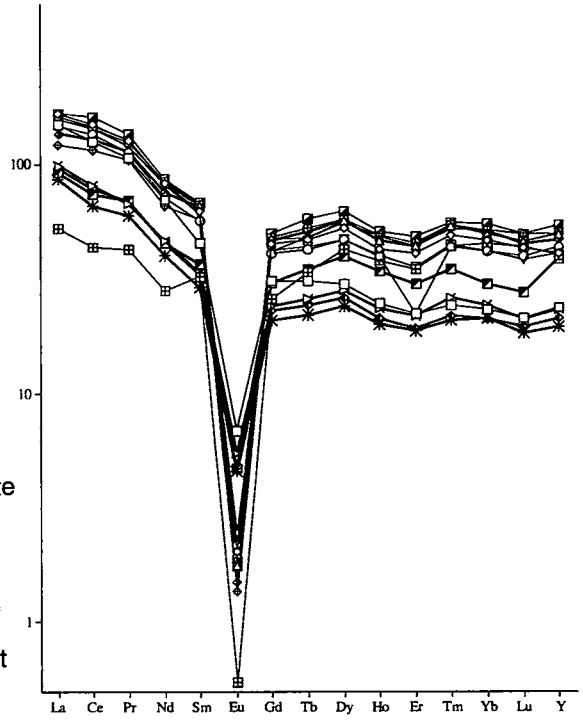

FIGURE 7: REE profile of the granite from the Selim granite. Note that all of the samples show tetrad REE patterns with huge negative anomalies. In all individual patterns, four elemental groups (La–Nd, Nd–Gd, Gd–Er, Er–Lu) form four distinct convex patterns.

Pluton Slim Sample No	Outer CH350	Outer CH800	Outer CH950	Outer CH1030	Inner CH1090	Inner CH1170	Inner CH1190	Inner CH1210	Inner CH1230	Inner CH1280	Outer CH3020	Outer CH3040	Outer CH3270	Outer CH3300	Outer CH3340
Major element in wt%															
SiO_2	75.61	75.34	76.18	76.15	76.76	75.8	75.37	75.39	77.12	75.94	75.19	74.45	76.89	74.26	75.87
TiO_2	0.25	0.1	0.1	0.1	0.03	0.06	0.11	0.14	0.1	0.11	0.19	0.2	0.17	0.18	0.16
Al_2O_3	12.85	12.43	13.04	12.4	13.04	13.04	12.78	12.96	12.53	12.99	13.01	13.49	11.95	13.56	12.68
Fe(tot)	1.66	1.24	1.18	1.28	0.79	1.12	1.14	1.21	1.04	1.72	1.55	1.68	1.54	1.66	1.61
MnO	0.03	0.04	0.04	0.04	0.03	0.04	0.04	0.04	0.03	0.04	0.04	0.04	0.02	0.04	0.04
CaO	0.71	0.36	0.51	0.39	0.33	0.42	0.47	0.23	0.1	0.46	0.38	0.52	0.31	0.55	0.35
K_2O	6.07	5.3	5.47	5.27	4.74	4.81	5.2	5.42	5.17	5.27	5.79	5.8	5.31	5.32	5.48
P_2O_5	0.07	0.02	0.02	0.02	0.01	0.01	0.01	0.01	0.02	0.01	0.12	0.12	0.1	0.12	0.14
MgO	0.24	0.01	0.03	0.01	0.01	0.01	0.04	0.01	0.01	0.01	0.19	0.15	0.05	0.14	0.11
Na_2O	2.55	2.94	3.16	2.93	3.71	3.52	3.16	3.28	2.87	3.26	2.93	2.75	2.52	3.02	2.49
Total	100.04	97.78	99.73	98.59	99.45	98.83	98.32	98.69	98.99	99.81	99.39	99.2	98.86	98.85	98.93
Trace element in ppm															
Ba	237	59	85	47	38.6	37.4	65.1	67.5	30.1	42.2	192	211	104	165	129
Nl	13.6	14.2	13.3	15.6	14.2	14.6	15.4	14.8	10.8	13.2	9.8	14.5	13	14.4	13.2
Pb	51	57.5	54.9	56.4	61.6	71.2	64.2	69.5	79.8	59	44.3	47.1	35	33	38.9
Rb	478	716	734	718	797	775	746	762	717	741	559	567	549	577	593
Sr	66.1	31.8	31.1	28.9	19.7	24.8	27.9	30.9	24.6	25.9	45	50.7	42.7	46.8	40.6
Th	55	52.5	46.6	49.4	19.2	40.5	44.4	46.7	44.5	40	39.4	43.3	40.1	37.9	39
V	11.9	9.9	6.8	5.4	8.5	8	7.9	8.4	7.8	7.9	11.8	10.2	6.5	11.7	7.5
Zr	146	107	96.8	105	53.2	89.3	99.4	101	103	96.5	113	128.4	107	112	107
Zn	27.9	29.2	30.2	29.7	21.9	54.6	30.9	37.4	42.5	27.9	29.8	30.9	16.4	28	26.4
Cu	5.7	3.5	4.8	4.4	2.9	9.1	4.9	4.5	6.7	5	4.9	3.95	3.7	4.9	4.4
Cr	191	199	149	210	194	211	155	205	166	179	184	216	177	184	204
Sc	6.3	5.4	6.3	5.6	5.9	4.6	5.1	6.3	5.8	5.4	6.9	5.15	4.8	5.7	3.9
Rare Earth Element in ppm															
La	50.7	56.2	50.2	54.5	18	41.2	53.2	55.2	56.5	46.8	29.3	33.7	31.5	32.7	29.3
Ce	115	136	123	133	40	105	130	130	146	117	60.3	73.8	68	71.3	60.9
Pr	129	15.3	13.7	15.5	5.19	12.7	15.1	14.6	16.4	13.8	7.31	8.18	8.42	8.38	7.63
Nd	45.1	53	46.1	53.3	18.1	42.6	54.4	52.5	55.7	48.9	25.8	29.7	29.3	29.3	26.5
Sm	8.9	12.3	11.1	13	6.3	11.3	13.1	12	13.3	12.8	5.72	6.56	7.16	6.49	6.02
Eu	0.51	0.15	0.16	0.13	0.04	0.1	0.14	0.18	0.13	0.11	0.34	0.41	0.35	0.35	0.29
Gd	8.07	11.8	10.7	12.4	6.72	10.9	12.5	11	13.1	12.1	5.44	6.24	7.88	5.98	5.57
Tb	1.47	2.22	2.02	2.24	1.59	2.26	2.5	2.06	2.73	2.41	1.04	1.22	1.64	1.14	1.06
Dy	9.06	15.9	14.2	17.2	12.9	16.8	17.3	14.1	18.9	17.2	7.2	8.46	11.9	7.85	7.24
Ho	1.95	3.35	3.09	3.65	2.97	3.8	3.83	3.14	4	3.65	1.56	1.84	2.68	1.68	1.55
Er	5.58	10.3	5.58	11.1	8.76	11.1	11.4	8.93	12.2	11.1	4.72	5.35	6.6	4.65	4.28
Tm	0.78	1.58	1.4	1.73	1.41	1.68	1.75	1.43	1.78	1.73	0.67	0.84	1.12	0.7	0.68
Yb	5.16	10.3	9.25	11	9.99	11.4	11.1	9.2	12.2	11.3	4.72	5.35	6.6	4.65	4.28
Lu	0.73	1.48	1.35	1.57	1.49	1.7	1.57	1.31	1.7	1.53	0.63	0.72	0.94	0.67	0.6

TABLE 1 : Represantative Major, Trace and REE elements of the of the Selim granite.

There are two arguments against it. (1) Water–rock interaction is a rather common phenomenon, but no REE tetrad effect has been identified in hydrothermally altered rocks which are not of highly evolved rocks. (2) Analyses on individual phases, such as rock forming (K-feldspar, biotite, garnet, blue amphibole) or accessory minerals (topaz, monazite, pyrochlore, xinanite, xenotime, apatite), also show the tetrad effect on all the phases (Irber, 1999). This feature is clearly magmatic, inherited from crystallization of melt with the tetrad effect already produced and hardly be formed by post-magmatic water–rock interaction.

ACKNOWLEDGEMENTS

This research was supported by University of Malaya grant FL 0727/2004A. The author thanks Prof Chen Tingyu for the rock analyses at the Academy of Institute of Geology Chinese Academy of Geological Sciences, Beijing for major, trace and REE analyses.

REFERENCES

AZMAN A GHANI. 2000a. The Western Belt granite of Peninsular Malaysia : some emergent problems on granite classification and its implication. Geosciences Jour. 4(4), 283-293.

AZMAN A GHANI. 2000b. Some 'I' type features in the so-called 'S' Western Belt granite. Bull. Geol. Soc. Malaysia 44, 133 - 138

BAU, M., 1996. Controls on the fractionation of isovalent trace elements in magmatic and aqueous systems: evidence from Y/Ho, Zr/Hf, and lanthanide tetrad effect. Contributions to Mineralogy and Petrology 123, 323–333.

CHAPPELL, B. W. AND WHITE, A. J. R., 1992. I- and S- type granites in the Lachlan fold belt. Trans. Roy. Soc. Edibn: Earth Sciences, 83,1- 26.

CHAROY, B AND RAIMBAULT, L., 1994. Zr-, Th- and REE-rich biotite differentiates in the A-type granite pluton of Suzhou (Eastern China): the key role of fluorine. J. Petrol. 35, 919–962

COBBING, E. J., PITFIELD, P. E. J., DARBYSHIRE, D. P. F., AND MALLICK, D. I. J. 1992. The granites of the South-East Asian tin belt. Overseas Memoir 10, B.G.S.

HUTCHISON, C. S., 1996. Geological evolution of South East Asia. Bull. Geol. Soc. Malaysia, 368 pp.

IRBER, W., 1999.The lanthanide tetrad effect and its correlation with K/Rb, Eu/Eu*, Sr/Eu, Y/Ho, and Zr/Hf of evolving peraluminous granite suites. Geochim. Cosmochim. Acta 63 489–508

BOR-MING JAHN, FUYUAN, W, CAPDEVILA, R, MARTINEAU, F, ZHENHUA, Z, YIXIAN W., 2001. Highly evolved juvenile granites with tetrad REE patterns: the Woduhe and Baerzhe granites from the Great Xing'an Mountains in NE China. Lithos 59, 171–198

LEE, S.G., MASUDA, A. AND KIM, H.S., 1994. An early Proterozoic leuco-granitic gneiss with the REE tetrad phenomenon. Chemical Geology 114, pp. 59–67.

LIEW, T.C., 1983. Petrogenesis of the Peninsular Malaysia granitoid batholiths. Unpubl. PhD thesis , Australia National University.

LIGGETT, D.L., 1990. Geochemistry of the garnet-bearing Tharps Peak granodiorite and its relation to other members of the Lake Kaweah intrusive suite, southwestern Sierra Nevada, California. In: Anderson, J.L., Editor, The Nature and Origin of Cordillera magmatism Geological Society of America Memoir 174, 225–236.

LONDON, D, 1986. Magmatic–hydrothermal transition in the Tanco rare-element pegmatite: evidence from fluid inclusions and phase-equilibrium experiments. Am. Mineral. 71, 376–395.

LONDON, D, 1987. Internal differentiation of rare-element pegmatites: effect of boron, phosphorus and fluorine. Geochim. Cosmochim. Acta 51 (1987), pp. 403–420.

LUDINGTON, S, 1981. The Redskin granite: evidence for thermo-gravitational diffusion in a Precambrian granite batholith. Jour. Geophy. Res., 86 (B11), 10423 - 10430.

MARUEJOL, P. CUNEY, M AND TURPIN, L.,1990. Magmatic and hydrothermal REE fractionation in the Xihuashan granites (SE China). Contrib. Mineral. Petrol. 104, 668–680.

YURIMOTO, H., DUKE, E.F., PAPIKE, J.J. AND SHEARER, C.K., 1990. Are discontinous chondrite-normalized REE patterns in pegmatitic granite systems the results of monazite fractionation?. Geochimica et Cosmochimica Acta 54, pp. 2141–2145.

ZHAO, Z.-H., MASUDA, A. AND SHABANI, M.B., 1993. REE tetrad effects in rare-metal granites. Chinese Journal of Geochemistry 12, pp. 206–219.

ZHAO, Z.-H., XIONG, X.-L. AND HAN, X.-D., 1999. The formation mechanism of REE tetrad in granites. Science in China (Ser. D) 29, pp. 331–338 (in Chinese)

Manuscript received 23 February 2005